The ancient Chinese civilization left remarkable signals in the marine environment since the Bronze Age

Xiang Sun
Fudan University https://orcid.org/0000-0001-7693-1125
Limin Hu (hulimin@fio.org.cn)
Ocean University of China
Bangqi Hu
Ocean University of China
Xueshi Sun
Fudan University
Xiao Wu
Ocean University of China
Naishuang Bi
Ocean University of China
Tian Lin
Shanghai Ocean University
Zhigang Guo
Fudan University
Zuosheng Yang
Ocean University of China

Article

Keywords: Civilization evolution in China, black carbon, soot signal, sedimentary record, Bronze Age

Posted Date: January 11th, 2021

DOI: https://doi.org/10.21203/rs.3.rs-143207/v1

The ancient Chinese civilization left remarkable signals in the marine environment since the Bronze Age

Xiang Sun[1,2], Limin Hu[2,3*], Bangqi Hu[2,4], Xueshi Sun[1], Xiao Wu[2,3], Naishuang Bi[2,3], Tian Lin[5], Zhigang Guo[1,2*], Zuosheng Yang[3]

[1] Department of Environmental Science and Engineering, Fudan University, Shanghai 200438, China

[2] Laboratory for Marine Geology, Qingdao National Laboratory for Marine Science and Technology, Qingdao 266061, China

[3] Key Laboratory of Submarine Geosciences and Prospecting Techniques, Ministry of Education of China, College of Marine Geosciences, Ocean University of China, Qingdao 266100, China

[4] Qingdao Institute of Marine Geology, Qingdao, 266071, China

[5] College of Marine Ecology and Environment, Shanghai Ocean University, Shanghai 201306, China

Corresponding authors: hulimin@ouc.edu.cn; guozgg@fudan.edu.cn

Abstract

To understand the onset of human civilization evolution recorded in the marine environment, a 6000-year record of black carbon (BC), including char and soot, was examined in a sediment core from the central South Yellow Sea. The results showed that the colder and drier climate dominated the variation in fire activity in northern

China after mid-Holocene via decreased precipitation and vegetation cover. The char released from the fire activity, can barely retrieve traces preserved in the marine sediments during the civilization evolution in China since ~1 ka BP. Fortunately, the soot-BC signal demonstrated that anthropogenic forces have overwhelmed the natural causes of soot emission since ~4 ka BP (Bronze Age) in northern China. The variation in soot closely matched periods when there was large-scale use of coal or charcoal after ~2 ka BP and when indigenous coking technology was promoted after ~1.3 ka BP, and times with low soot abundance coincided with periods of social unrest. This work provides evidence that the soot signal could be a robust tracer for tracking the civilization evolution, and the ancient Chinese civilization left remarkable soot signals in the marine environment since the Bronze Age.

Key words: Civilization evolution in China, black carbon, soot signal, sedimentary record, Bronze Age

1. Introduction

Industrialization is a revolutionary stage in the civilization evolution because it has changed the lifestyle of human beings and brought great conveniences to human life (1). However, the scale of carbon emissions since the industrial revolution have led to a rise in atmospheric greenhouse gases at an unprecedented rate due to the large-scale use of fossil fuels (*e.g.*, petroleum and coal) (2), which has significantly affected the surface ecosystems (3), the atmospheric chemical composition (4), and even the regional and global climate (5). The energy structures always link to the civilization evolution since humans could use fire by biomass fuels as early as the middle Pleistocene (6, 7). However, the visible trace for the onset of the ancient human civilization in the environment is poorly constrained, which varies spatially over the earth and represents a key piece of information to the concept of the Anthropocene (2).

Black carbon (BC) is a highly aromatic, recalcitrant carbon species released both from the wildfire and anthropogenic fire for the main energy utilization in ancient human civilization. It has two subtypes, char and soot (8, 9), which can be distinguished by thermal optical reflectance due to their different burning temperatures (10, 11). BC is widely distributed in lake and ocean sediments via transportation by atmospheric circulation and surface runoff (12). Char particles (1~100 μm) are residues of combustion at temperatures of 300~600°C that retain some of the morphological and structural features of their precursors, and are a function of biomass burning. Soot particles (< 1 μm) are produced during high-temperature combustion (> 600°C), which is strongly related to anthropogenic fuels (*e.g.*, petroleum, coal, and charcoal) or high-intensity biomass burning (8, 9, 10, 13, 14, 15). The sedimentary records of char and soot can provide information for tracking past changes in fire activity forced by climate change or human activities on multi-decadal to millennial scales (16). For example, the char/soot ratio in sediment cores from the eastern China marginal seas was used to reconstruct the variation in the energy structures in China over the last 200 years (9), and char has been used to track fire activities during the Holocene in Africa (12), the Pacific Islands (17), Europe (18), and North America (19).

From the time when human beings use fire by biomass fuels as early as the middle Pleistocene to the period of the large-scale use of fossil fuels in the industrial revolution, there have been several stages in the evolution of human civilization, Neolithic Age, Bronze Age, and Iron Age. Sediment cores provides striking evidence of past contamination linked to the civilization evolution in various continents during human history (9, 20). Northern China is the birthplace of Chinese civilization, which is one of the oldest human civilizations. Therefore, this is a unique area for tracing civilization evolution in the environment. Studies on the historical records in the sedimentary strata for China have concentrated on fire activity in the large river basins in southern China (20) or examined local scales (15, 21, 22) associated with climate change and human activity, while seldom on the time node of civilization evolution in China.

The South Yellow Sea (SYS) lies in the path of the East Asian continental outflow driven by the East Asian winter monsoon (EAWM). It can receive and preserve large amounts of land-based materials from northern China as a natural archive via atmospheric deposition and ocean current transportation (23). Therefore, this is a unique and ideal place for tracing the civilization evolution in northern China. This work establishes a 6000-year high-resolution BC (char and soot) record from sediment core ZY2, taken from the central SYS, to reveal the fire history of a large-scale northern China since the mid-Holocene by exploring the relative importance of climate change and human activity, and trace the human civilization evolution in China. This reveals that the evolution of human civilization in China left remarkable signal in the marine sediment since the Bronze Age.

2. Materials and Methods

2.1. Study area and sampling

The SYS is a semi-closed marginal sea in the western Pacific located between China and the Korean Peninsula (Fig. 1). It is indirectly influenced by the Yellow and Yangtze Rivers (24). Under the influence of the EAWM, the SYS is downwind of the Asian continental outflow in spring and winter (25), and large amounts of land-based materials are deposited in the marginal seas (26–28). Sediment core ZY2 (35°31′N, 122°39′E) was collected in the SYS at a water depth of 68.5 m from the R/V Dong-Fang-Hong 2 in 2006. It is 342 cm long. The core was sampled at 1 cm intervals and kept at −20°C. The lithology and chronology of the core were reported previously (24). The age at the bottom of the core is ~6.2 ka BP, which is roughly when the modern current circulation of the Yellow Sea developed (29). The homogeneous gray, dark gray clayey silt of the core promised a stable sedimentary environment with sufficient sediment supply (24).

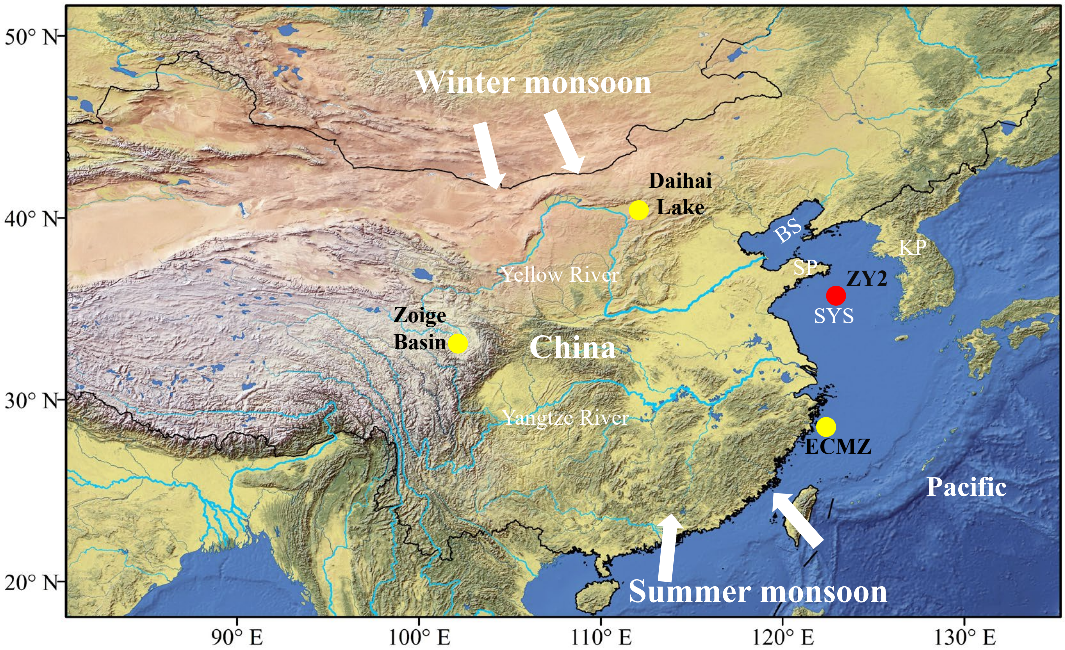

Fig. 1. A map showing the winter and summer monsoons, Bohai Sea (BS), South Yellow Sea (SYS), Yellow and Yangtze Rivers, Pacific Ocean, Korean (KP) and Shandong (SP) Peninsulas, ZY2 sediment core (red circle), and locations of fire-record sediment core studied previously (yellow circles) (20, 21, 22).

2.2. BC analysis

The abundance of BC was analyzed in 300 samples, at 1-cm intervals in the first 258 cm of the core and 2-cm intervals thereafter. The pretreatment method followed Fang *et al*. (2018) (9). BC was measured at Lanzhou Institute of Arid Meteorology, China Meteorological Administration using a thermal/optical carbon analyzer (DRI Model 2001A; American Desert Research Institute, Reno, NV, USA), which adopted the interagency monitoring of protected visual environment (IMPROVE) protocol. To begin, the analyzer oven was heated to 550°C in 100% He. This was switched to an O_2/He mixture (2%/98%) and the oven was heated from 550°C to 700°C and then to 800°C. The gas generated with these temperature gradients was catalytically oxidized to CO_2 in an oxidation furnace (MnO_2), and then converted into CH_4 in a reducing environment. The carbon content was measured with a flame ion detector, which has three peaks corresponding to organic carbon, char, and soot at three temperature stages (550, 700, and 800°C). BC equals the sum of char and soot (10) and is expressed in mg/g dry sediment. Replicate analyses showed that the relative error was within 5%, and the total carbon content of the blank filter sample was below 0.05 mg.

3. Results

The BC in sediment core ZY2 ranged from 2.1 to 3.7 mg/g (mean 3.1 ± 0.31 mg/g; 1σ; n = 300), and increased slightly from ~6.2 to 4.0 ka BP and subsequently decreased. This showed a series of centennial to multi-centennial fluctuations, with an obvious decrease at ~1 ka BP (Fig. 2a). The char (range 2.0–3.5 mg/g, mean 3.0 ± 0.31 mg/g; 1σ; n = 300) showed a similar trend to BC (Fig. 2b). The detrend char result (Fig. 2d) obtained by 50% loess regression (to present the char variation on a centennial timescale) showed no significant periodicity in a spectral analysis with a multi-taper method and wavelet transform analysis. The strong correlation between char and BC (R^2

= 0.99, $P < 0.01$, n = 300) and the lack of a correlation ($R^2 = 0.020$, $P = 0.014$, n = 300) between soot and BC suggested that char is the main component of BC. The soot abundance (range 0.14–0.31 mg/g, mean 0.19 ± 0.025 mg/g; 1σ; n = 300) increased slightly at mid-Holocene (Fig. 2c), similar to the char variation at that time. The soot abundance variation was distinct from that of char after ~4 ka BP, with a pronounced increasing trend at ~2 ka BP and a downtrend at ~1.3 ka BP (Fig. 2c).

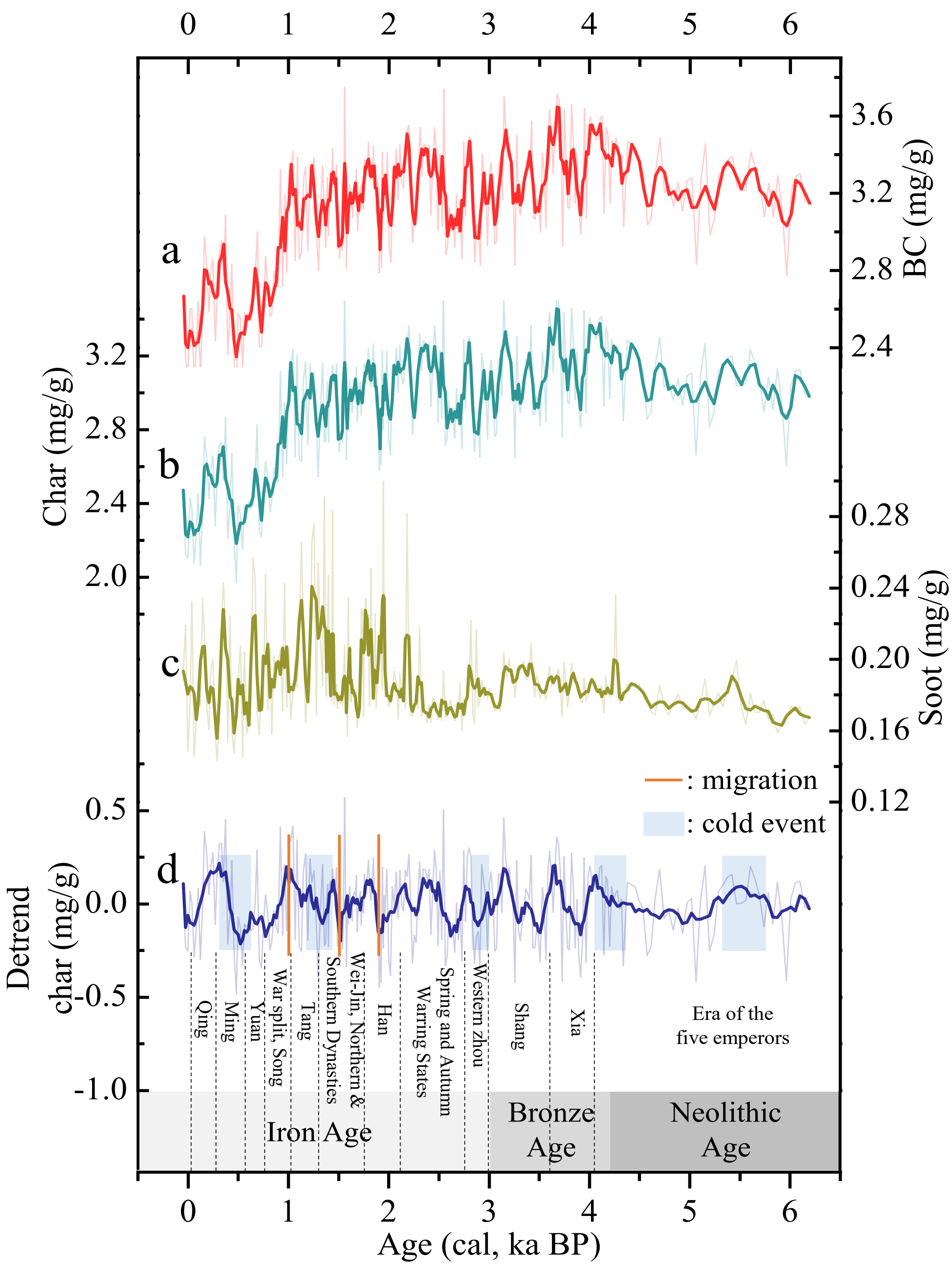

Fig. 2. Sediment BC data for core ZY2 since ~6.2 ka BP: the variation in (a) BC, (b) char, and (c) soot; (d) the char detrend with 50% loess regression (Fig. S1). Signal smoothing averaging three adjacent points for (a) to (c), and seven points for (d).

4. Discussion

4.1. The climate change dominated the variations of char

The similar production processes shared by BC (including char and soot) and polycyclic aromatic hydrocarbons (PAHs) could result in inference with BC sources by the signatures of PAHs (30-32). The source pattern of pyrogenic high-ring PAHs in the Yellow Sea sediments compared well with that of aerosol $PM_{2.5}$ (*i.e.*, particles with an aerodynamic diameter < 2.5 μm) collected upwind from northern Chinese cities, Beijing and Qingdao, demonstrating the significant influence of atmospheric deposition on the input of combustion-derived substances into the marginal sea off northern China (25). Moreover, the atmospheric deposition of BC contributed ~51% to the total input of BC in the Bohai Sea and more than that in the SYS (23). Thus, EAMW-forced atmospheric deposition played a dominant role in the BC input in the SYS. The history of the EAWM intensity has been reconstructed by analyzing the sensitive grain size (24). The lack of a correlation between the abundance of BC and grain size ($R^2 = 0.015$, $P < 0.05$, n = 300) suggests that the intensity of the EAWM was not the dominant factor causing the variations in BC (both char and soot) (char: $R^2 = 0.011$, $P = 0.058$; soot: $R^2 = 0.068$, $P < 0.01$). Additionally, the absence of a correlation between the abundance of BC and the clay, silt, and sand contents suggests that the BC abundance was not influenced by the dilution effects of other sediment fractions. Therefore, the sedimentary records of BC in sediment core ZY2 closely reflect the emissions due to fires in northern China.

The general decline in fire activity recorded by the char in core ZY2 (Fig. 3a) is consistent with char or BC records from sediment cores from the inner shelf of the East China Sea (20), the Zoige Basin in the eastern Tibetan Plateau (22), and Lake Daihai in north-central China (15, 21) (Fig. 1, Fig. S2). This suggests that the gradual weakening in fire activity since the mid-Holocene is a common phenomenon across the monsoon region of China. In the mid-Holocene, in the Northern Hemisphere, the earth was near its perihelion in the summer, which would result in a stronger radiation (33) and a greater land–ocean thermal contrast, thus increase temperature gradients, and strengthen the Asian Summer Monsoon (34). With the precession cycle, the earth gradually approached its apogee in summer in the Northern Hemisphere in the late Holocene (33). The earth's orbit decreased summer insolation in the Northern Hemisphere (Fig. 3b) (35) and induced the Asian Summer Monsoon. Oxygen isotopes are used to track past summer monsoons and the precipitation intensity (36). Stalagmite $\delta^{18}O$ in Dongge and Sanbao Caves in China shows a gradual increase since ~7 ka BP (36, 37), indicating gradual weakening of the precipitation since the mid-Holocene. Simultaneously, the temperature (Fig. 3d) (38), moisture (Fig. 3c) (39), and vegetation cover (Fig. 3e) (40) in northern China showed downward trends.

In general, lower temperatures are associated with decreased fire activity via vegetation productivity and the incidence of fire-promoting climate conditions (41). However, the char value of sediment core ZY2 unexpectedly increased slightly from

~6.2 to 4.0 ka BP (Fig. 3a) when the climate became colder and drier. Note that fire activity is not only associated with temperature but also with vegetation cover and precipitation. Pollen analyses of boreholes from the Yellow River Delta showed that evergreen and broadleaved deciduous forest thrived in northern China (indicated by high *Quercus*, *Carpinus*/*Ostrya*, and *Ulmus*/*Zelkova* pollen counts) from 9.8 to 4.5 ka BP in a warmer, wetter climate, and a significant reduction in deciduous *Quercus* pollen and an increase in conifer *Pinus* pollen at ~4 ka BP corresponded to a drier climate (42). Moreover, the percentage of tree pollen in a profile from Lake Daihai (north-central China) showed a clear downward trend since the mid-Holocene (Fig. 3e) (39, 40).

Additionally, the decrease in precipitation not only affected the vegetative cover (fuel abundance) but also increased its flammability (41). Fire responds differently to precipitation and depends on whether vegetation cover (fuel abundance) is initially a factor limiting fire spread. In arid and semi-arid environments, increases in precipitation tend to increase fires (43), whereas increased precipitation reduces fire activity in humid environments (44). Therefore, the unexpected increase in fire activity from ~6.2 to 4.0 ka BP could be attributed to a threshold effect of precipitation and vegetation cover on fire activity. Specifically, in the mid-Holocene, when northern China had a humid environment and vegetation cover (fuel abundance) was not a factor limiting fire spread, decreases in precipitation could enhance the flammability of vegetation and increase fire activity. Subsequently, as precipitation continued to decrease, the amount of vegetation decreased and limited fire propagation. This induced the decrease in fire activity with the continuous reduction in precipitation and vegetation since ~4 ka BP (Fig. 3a).

Although the millennial-scale, large-area decrease in fire activity in northern China since ~4 ka BP can be explained by the natural climate dynamics (45), the evolution of human civilization should not be ignored in this process (46). The Zhoukoudian archaeological discovery illustrated that Beijingers had the ability to control fire behavior as early as the middle Pleistocene (7). Since then, fire has been used for heating, lighting, cooking, driving beasts, living in groups, and making and creating new living materials (47). The Yellow River Basin in northern China is the origin of the ancient Chinese civilization and millet agriculture. Millet agriculture was developed in the pre-Yangshao Period (8.5~7 ka BP) (48), and fire has been used to clear forest for cultivation and settlement since ~7.7 ka BP in China (47). Subsequently, millet agriculture developed rapidly in the Yellow River Basin (49). The number of archaeological sites in northern China increased substantially after ~7 ka BP and even more markedly between ~4.5 and 3 ka BP (Fig. 3f) (50). However, the number of archaeological sites in northern China declined sharply at ~3 ka BP, which may be related to climate change and the growth characteristics of millet, which is a drought-tolerant crop that is sensitive to temperature change (48). The gradually weakened insolation and decreased temperature in the Northern Hemisphere is not always conducive to millet cultivation. The decrease in archaeological sites after ~3 ka BP (Fig.

3f) corresponded to a major shift in the subsistence economy from predominantly animal husbandry and plant cultivation to mobile pastoralism across present-day semiarid northern China, which left fewer traces in the archaeological records than sedentary communities (51). This variation in human activity (number of archaeological sites) was not recorded by the char in core ZY2, suggesting that climate change was the dominant factor affecting fires on a millennial-scale over a large area, rather than human activity. However, there has a more pronounced decrease in fire activity at ~1 ka BP (Fig. 3a), when a semi-pastoral, semi-agricultural economy was established in northern China to accommodate the cold-dry climate (52), and fire management was used to prevent uncontrolled wildfires to limit damage to settlements and agricultural resources (53), which might have led to the obvious decrease in fire activity at ~1 ka BP.

The record of fire based on char in core ZY2 also showed a series of centennial to multi-centennial fluctuations (Fig. 2d). The North Atlantic cold events (5.5, 4.2, 2.8, 1.4, and 0.4 ka BP) during the mid-late-Holocene (54, 55) were large-scale phenomena rather than local ones (56). Most of them could be attributed to weakening solar activity, which in turn affected the ocean and atmospheric circulation on earth, causing abrupt climate change (57, 58). The period of abrupt change corresponds to the variation in the Holocene Asian Summer Monsoon (36), which could have affected the fire activity in northern China. The detrend char records showed that the 5.5 and 4.2 ka BP cold events coincided with episodes of high fire activity; while the cold events of

2.8 and 1.4 ka BP and the Little Ice Age (~0.4 ka BP) were periods of low fire activity (Fig. 2d). This means that the threshold effect (as discussed above) of climate change on fire activity could also partly explain the centennial fluctuations in fire in northern China, suggesting that the cold events before ~4 ka BP promoted fire activity, while subsequent cold events decreased the fire activity.

The paleoclimatic and archaeological evidence suggests that the abrupt droughts and cold climate resulted in warfare, population migration, and dynasty change (59). This is especially true for northern China, where society was more sensitive to severe climatic conditions due to the relatively high latitudes (60). There were three large population migrations from northern to southern China during 1.9–1.8 ka BP (late Han Dynasty), 1.6–1.4 ka BP (Wei-Jin Southern & Northern Dynasties), and 1.1–0.9 ka BP (Tang-Song Dynasty) (61). The reduction in the population of northern China generally reduced the intensity of human activity, which decreased fire activities (20). The migrations in 1.9–1.8 and 1.6–1.4 ka BP coincided with low fire activity (Fig. 2d); while the migration in 1.1–0.9 ka BP coincided with high fire activity (Fig. 2d). The Tang-Song period occurred during the Medieval Warm Period, which likely overwhelmed the population reduction in northern China and dominated fire occurrence in this period.

Different spatial scales have different fire regimes. The climate–vegetation relationship can generally drive both global and sub-continental fire regimes, while human-induced fires are prominent mainly on a local scale (62-64). Small-scale human activity can affect natural fire regimes, even in pyrogeographic settings in which climate exerts strong, top-down controls on fuel (65). Fortunately, muddy shelf areas may contain an integrated burning imprint of the mainland, which avoids the influence of small-scale human activities on local fires. The discussion above means that variations of char are dominated by climate change, both on the millennium timescale and the centennial timescale. Even if the obvious decrease in fire activity at ~1 ka BP could attribute to the establishment of the semi-pastoral, semi-agricultural economy and the fire management in northern China, it was ultimately associated with the cold-dry climate. Therefore, char can barely retrieve traces left in the environment during the civilization evolution in China.

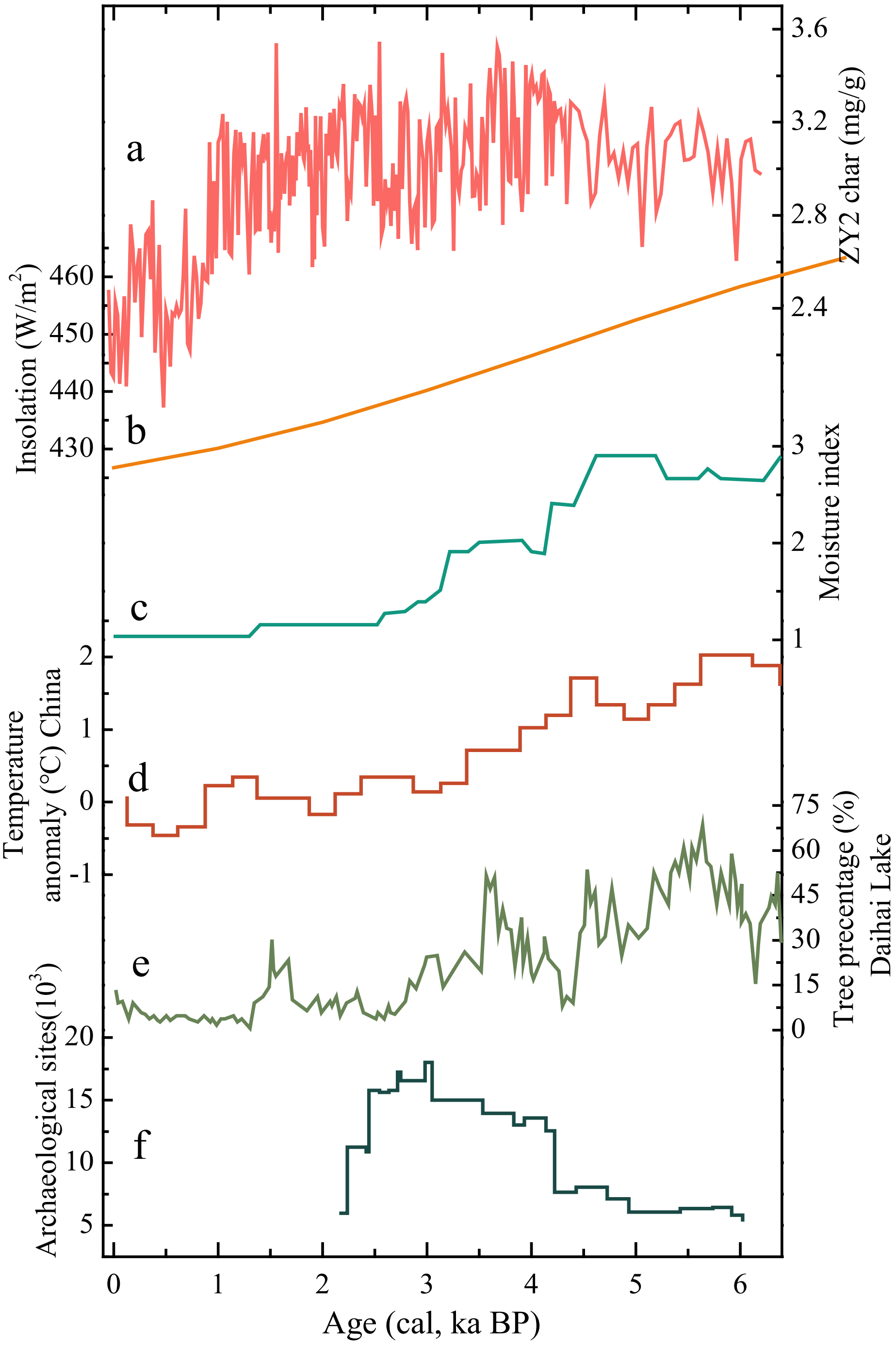

Fig. **3**. Comparison of the millennial-timescale variation in BC records from ZY2 with other records since 6.2 ka BP. (a) Fire activities recorded by char from core ZY2 in the SYS (this study); (b) extraterrestrial insolation of mid-month insolation 65N for July (33); (c) moisture index-based pollen in northern China (39); (d) temperature anomaly in China (38); (e) percentage of tree pollen recorded from the sediment core in Lake Daihai (40); (f) change in the total number of archaeological sites in northern China from 6 to 2 ka BP (50).

4.2. The soot variation footprint the ancient civilization evolution in China

The soot abundance increased slightly during the mid-Holocene (Fig. 2c), similar to the char variation at that time. The correlation between soot and char at 4~6.2 ka BP was significant (Fig. 4a; $R^2 = 0.46$, $P < 0.01$, n = 58; removing two outliers, Fig. S3). Soot is produced via high-temperature (> 600°C) gas-to-particle conversion under dry conditions and can reflects high-intensity biomass burning and is generated with char (14). Therefore, the slight increase in soot during the mid-Holocene could be predominantly attributed to natural factors. However, the correlation between soot and char decreased during 3~4 ka BP (Fig. 4b; $R^2 = 0.33$, $P < 0.01$, n = 60) and showed no correlation after ~3 ka BP (Fig. 4f), suggesting the influence of anthropogenic factors on soot emission. Besides release from high-intensity biomass burning, soot can be generated from the combustion of fuel (*e.g.*, petroleum, coal, and charcoal) (13, 14). Although the Hou Hanshu, a famous Chinese historical document about the Han Dynasty, indicates that China first collected and used petroleum in the Wei-Jin, Southern & Northern Dynasties (1730–1369 BP), petroleum was not used widely (66). However, China has long used coal and charcoal as an important source of energy (67).

The Xia Dynasty, the first Chinese dynasty, was established more than 4000 years ago, when China entered the Bronze Age. Bronze is an alloy of copper and tin or lead. Its melting point is between 700 and 900°C, which exceeds the production temperature of soot (> 600°C). At that time, charcoal and bamboo charcoal were the major fuels for smelting bronze (68). At smelting temperatures, charcoal fuel promoted soot production, which caused the increase in soot during 3~4 ka BP (Fig. 4g). The anthropogenic soot emissions reduced the correlation between soot and char during 3~4 ka BP (Fig. 4f).

China entered the Iron Age during the Western Zhou Dynasty (~3 ka BP). The smelting temperature of iron is about 1500°C, meaning that more fuel is used for smelting (68). During the Iron Age, soot and char were not correlated, suggesting that anthropogenic factors dominated soot emission. Soot abundance increased at ~2 ka BP (Fig. 4g), corresponding to the Han Dynasty (2156–1730 BP), when coal and charcoal fuel began to be used for large-scale metal smelting and agricultural tool production (67, 68). The Song Dynasty (990–671 BP) started a national coal monopoly, and coal became an important resource related to the national economy and people's livelihoods during the Ming and Qing Dynasties (582–39 BP) (67, 69). However, soot abundance decreased beginning in ~1.3 ka BP (Fig. 4g), when indigenous coking technology was developed (70). In the Tang Dynasty (1332–1043 BP), coke was in its embryonic stage. By the Song Dynasty (990–671 BP), coking technology had matured and coke ovens were studied in archeology (70). In indigenous coking technology, a kiln with an ignition hole in the side wall is used to ignite the coking coal stacked in the kiln. This suggests that the application of indigenous coking technology reduced the emission of soot compared with the direct combustion of raw coal.

China underwent several dynasty changes and united and split after the Xia Dynasty (4096~3625 BP). The Spring and Autumn Waring States (2721–2171 BP), Wei-Jin Southern & Northern Dynasties (1730–1369 BP), and Five Dynasties & Ten Kingdoms (1043–971 BP) periods were the three main splits in Chinese history, corresponding to the main three valleys in soot abundance at ~2.5, ~1.5, and ~0.8 ka BP (Fig. 4g). Periods with low soot abundance generally coincided with dynasty changes (Fig. 4g), when there were more wars. During periods of social stability, coal and charcoal were the main energy source for agricultural tool and handicraft production, metal smelting, and heating (68). Wars led to social unrest and the displacement of people, reducing soot emissions from coal and charcoal use in people's daily lives.

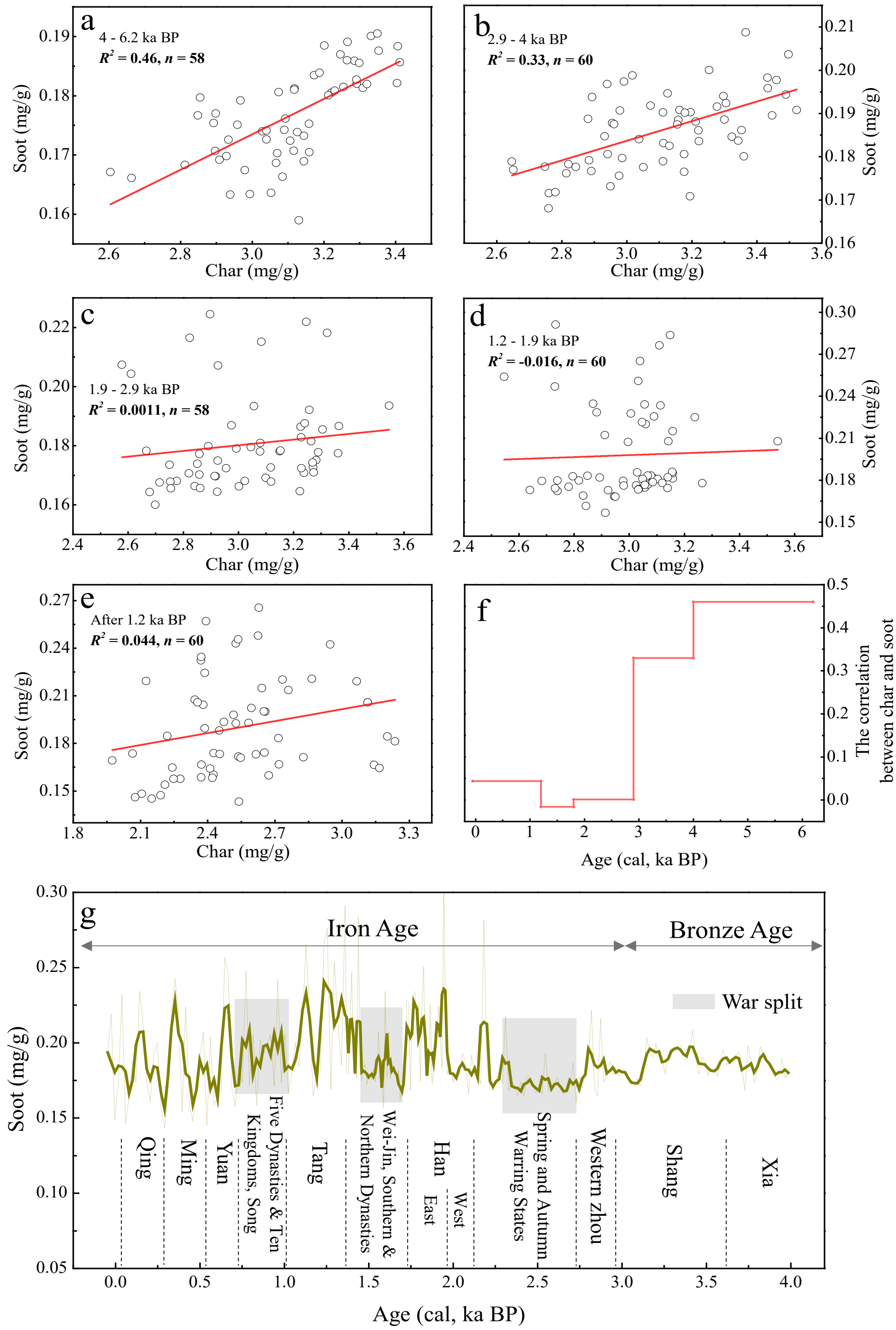

Fig. 4. (a) to (e) show the correlations between char and soot at 0.05–1.2, 1.2–1.88, 1.88–2.9, 2.9–4, and, 4–6.2 ka BP, respectively. (f) Change in the correlation between char and soot since ~6.2 ka BP; (g) changes in soot from 0 to 4 ka BP and the corresponding Chinese dynasties; signal smoothing was performed by averaging three adjacent points.

5. Conclusions and Implications

The char-BC record revealed that the colder, drier climate before ~4 ka BP enhanced the fire activity slightly; this was followed by an obvious reduction in fire activity. The decoupling between climate change and fire occurrence suggested that the climate-induced precipitation and vegetation cover had a threshold effect on the fire regime. The synergistic effect of human activity and climate change resulted in a significant decline in fire ~1ka BP. Ultimately, the climate dominated the variation in fire activity in northern China both on the millennium timescale and the centennial timescale, therefore the char can barely retrieve traces persevered in the marine environment during the civilization evolution in China. However, the variation in soot clearly marked the large-scale use of coal and charcoal since ~2 ka BP (Han Dynasty) and adoption of indigenous coking technology after ~1.3 ka BP (Tang Dynasty), which is consistent with historical documents and archaeological discoveries. Periods of social unrest in the cold weapon era coincided with the low soot abundance, suggesting that wars reduced in soot emission from coal and charcoal use in people's daily lives. The soot signal demonstrated that anthropogenic forces overwhelmed natural factors as the cause of soot emissions after ~4 ka BP (Bronze Age) in northern China. The time node represents a key piece of information to establish the natural background of soot-BC in the marine sediments and to specify the concept of the Anthropocene.

Acknowledgments

This work was supported by the National Natural Science Foundation of China (NSFC) (Nos.: 41676034 and 41722603), the National Key Research and Development Program of China (No: 2016YFA0601903) and in part by the Taishan Scholar Program (TSQN20182117).

The English in this document has been checked by at least two professional editors, both native speakers of English. For a certificate, please see: http://www.textcheck.com/certificate/YRNO5t

References:

1. S. Lall, Technological capabilities and industrialization. World Development **20**, 165-186 (1992).

2. A. Glikson, Fire and human evolution: The deep-time blueprints of the Anthropocene. Anthropocene **3**, 89-92 (2013).

3. B. Bond-Lamberty, S. D. Peckham, D. E. Ahl, S. T. Gower, Fire as the dominant driver of central Canadian boreal forest carbon balance. Nature **450,** 89-90 (2007).

4. F. Justino, W. R. Peltier, H. A. Barbosa, Atmospheric susceptibility to wildfire occurrence during the Last Glacial Maximum and mid-Holocene. Palaeogeography Palaeoclimatology Palaeoecology **295,** 76-88 (2010).

5. M. J. S. B. David et al., Fire in the earth system. Science **324**, 481-484 (2009).

6. J. R. Marlon et al., Global biomass burning: a synthesis and review of Holocene paleofire records and their controls. Quaternary Science Reviews **65,** 5-25 (2013).

7. S. Weiner, Q. Xu, P. Goldberg, J. Liu, O. Bar-Yosef, Evidence for the Use of Fire at Zhoukoudian, China. Science **281,** 251-253 (1998).

8. M. Elmquist, G. Cornelissen, Z. Kukulska, O. Gustafsson, Distinct oxidative stabilities of char versus soot black carbon: Implications for quantification and environmental recalcitrance. Global Biogeochemical Cycles **20**, GB20092 (2006).

9. Y. Fang et al., Spatiotemporal trends of elemental carbon and char/soot ratios in five sediment cores from eastern China marginal seas: Indicators of anthropogenic activities and transport patterns. Environmental Science & Technology **52,** 9704-9712 (2018).

10. Y. M. Han et al., Evaluation of the thermal/optical reflectance method for discrimination between char- and soot-EC. Chemosphere **69,** 569-574 (2007).

11. C. Santin, S. H. Doerr, C. M. Preston, G. Gonzalez-Rodriguez, Pyrogenic organic matter production from wildfires: a missing sink in the global carbon cycle. Global Change Biology **21,** 1621-1633 (2015).

12. M. I. Bird, J. A. Cali, A million-year record of fire in sub-Saharan Africa. Nature **394,** 767-769 (1998).

13. Y. M. Han et al., Asian inland wildfires driven by glacial-interglacial climate change. Proceedings of the National Academy of Sciences **117**, 5184-5189 (2020).

14. Y. M. Han et al., Climate and fuel controls on north American paleofires: Smoldering to flaming in the late-glacial-Holocene transition. Science Reports **6**, 20719 (2016).

15. Y. M. Han, J. R. Marlon, J. J. Cao, Z. D. Jin, Z. S. An, Holocene linkages between char, soot, biomass burning and climate from Lake Daihai, China. Global Biogeochemical Cycles **26**, GB4017 (2012).

16. V. Iglesias, C. Whitlock, Fire responses to postglacial climate change and human impact in northern Patagonia (41–43°S). Proceedings of the National Academy of Sciences **111,** 5545-5554 (2014).

17. D. B. McWethy et al., Rapid landscape transformation in South Island, New Zealand, following initial Polynesian settlement. Proceedings of the National Academy of Sciences **107**, 21343-21348 (2010).

18. F. Olsson, M. Gaillard-Lemdahl, G. Lemdahl, A. Eklund, P. Lanos, Holocene forest fires in the hemiboreal zone of southern Sweden 10,500 calendar years BP to modern time: The role of climate and human activities. Paleogeography, Paleoclimatology, Paleoecology **291**, 128-141 (2010).

19. C. Carcaillet, P. J. H. Richard, H. Asnong, L. Capece, Y. Bergeron, Fire and soil erosion history in East Canadian boreal and temperate forests. Quaternary Science Reviews **25**, 1489-1500 (2006).

20. W. Pei et al., Human impact overwhelms long-term climate control of fire in the Yangtze River Basin since 3.0 ka BP. Quaternary Science Reviews **230,** 106165 (2020).

21. X. Wang, J. Xiao, L. Cui, Z. Ding, Holocene changes in fire frequency in the Daihai Lake region (north-central China): indications and implications for an important role of human activity. Quaternary Science Reviews **59,** 18-29 (2013).

22. W. Zhao, Y. Zhao, F. Qin, Holocene fire, vegetation, and climate dynamics inferred from charcoal and pollen record in the eastern Tibetan Plateau. Journal of Asian Earth Sciences **147,** 9-16 (2017).

23. Y. Fang et al., Flux and budget of BC in the continental shelf seas adjacent to Chinese high BC emission source regions. Global Biogeochemical Cycles **29,** 957-972 (2015).

24. B. Hu et al., Grain size records reveal variability of the East Asian Winter Monsoon since the Middle Holocene in the Central Yellow Sea mud area, China. Science China-earth Sciences **55,** 1656-1668 (2012).

25. T. Lin et al., Sources of polycyclic aromatic hydrocarbons to sediments of the Bohai and Yellow Seas in East Asia. Journal of Geophysical Research: Atmospheres **116,** D23305 (2011).

26. J. M. Martin, J. Zhang, M. C. Shi, Q. Zhou, Actual flux of the huanghe (Yellow-river) sediment to the western Pacific-ocean. Netherlands Journal of Sea Research **31,** 243-254 (1993).

27. J. D. Milliman, Y. S. Qin, M. E. Ren, Y. Saito, Mans influence on the erosion and transport of sediment by asian rivers - the Yellow-river (Huanhe) example. Journal of Geology **95,** 751-762 (1987).

28. C. R. Alexander, D. J. Demaster, C. A. Nittrouer, Sediment Accumulation in a modern epicontinental-shelf setting - the yellow sea. Marine Geology **98,** 51-72 (1991).

29. J. M. Kim, M. Kucera, Benthic foraminifer record of environmental changes in the Yellow Sea (Hwanghae) during the last 15,000 years. Quaternary Science Reviews **19,** 1067-1085 (2000).

30. Y. M. Han et al., Comparison of elemental carbon in lake sediments measured by three different methods and 150-year pollution history in eastern China. Environmental Science & Technology **45,** 5287-5293 (2011).

31. Y. M. Han et al., Stronger association of polycyclic aromatic hydrocarbons with soot than with char in soils and sediments. Chemosphere **119,** 1335-1345 (2015).

32. Y. Fang et al., Application of PMF receptor model merging with PAHs signatures for source apportionment of black carbon in the continental shelf surface sediments of the Bohai and Yellow Seas, China. Journal of Geophysical Research: Oceans **121,** 1346-1359 (2016).

33. A. Berger, M. F. Louter, Insolation values for the climate of the last 10000000 years. Quaternary Science Reviews **10,** 297-317 (1991).

34. J. E. Kutzbach, Climatic changes of the last 18,000 years - observations and model simulations. Science **241,** 1043-1052 (1988).

35. A. K. Gupta, D. M. Anderson, J. T. Overpeck, Abrupt changes in the Asian southwest monsoon during the Holocene and their links to the North Atlantic Ocean. Nature **421,** 354-357 (2003).

36. Y. Wang et al., The Holocene Asian Monsoon: links to solar changes and North Atlantic climate. Science **308,** 854-857 (2005).

37. Y. Wang et al., Millennial- and orbital-scale changes in the East Asian monsoon over the past 224,000 years. Nature **451,** 1090-1093 (2008).

38. S. Wang, D. Gong, J. Zhu, Twentieth-century climatic warming in China in the context of the Holocene. Holocene **11,** 313-321 (2001).

39. Y. Zhao, Z. Yu, F. Chen, J. Zhang, B. Yang, Vegetation response to Holocene climate change in monsoon-influenced region of China. Earth-Science Reviews **97,** 242-256 (2009).

40. J. Xiao, Q. Xu, T. Nakamura, X. Yang, W. Liang, Y. Inouchi, Holocene vegetation variation in the Daihai Lake region of north-central China: a direct indication of the Asian monsoon climatic history. Quaternary Science Reviews **23,** 1669-1679 (2004).

41. A. L. Daniau et al., Predictability of biomass burning in response to climate changes. Global Biogeochemical Cycles **26**, GB4007 (2012).

42. S. Yi, Y. Saito, H. Oshima, Y. Q. Zhou, H. L. Wei, Holocene environmental history inferred from pollen assemblages in the Huanghe (Yellow River) delta, China: climatic change and human impact. Quaternary Science Reviews **22,** 609-628 (2003).

43. T. T. Veblen, T. Kitzberger, Inter-hemispheric comparison of fire history: The Colorado front range, U.S.A., and the northern Patagonian Andes, Argentina. Plant Ecology **163,** 187-207 (2002).

44. M. A. Krawchuk, M. A. Moritz, Constraints on global fire activity vary across a resource gradient. Ecology **92,** 121-132 (2011).

45. T. Kleinen, P. Tarasov, V. Brovkin, A. Andreev, M. Stebich, Comparison of modeled and reconstructed changes in forest cover through the past 8000 years: Eurasian perspective. The Holocene **21,** 723-734 (2011).

46. F. H. Chen et al., Asian dust-storm activity dominated by Chinese dynasty changes since 2000 BP. Nature Communications **11**, 992 (2020).

47. Y. Zong et al., Fire and flood management of coastal swamp enabled first rice paddy cultivation in east China. Nature **449,** 459-U4 (2007).

48. X. Yang et al., Early millet use in northern China. Proceedings of the National Academy of Sciences **109,** 3726-3730 (2012).

49. G. Dong, S. Zhang, Y. Yang, J. Chen, F. Chen, Agriculture intensification and its impact on the environment in the Neolithic Age of northern China. Scientific Bulletin (in Chinese) **61**, 2913-2925 (2016).

50. M. Wagner et al., Mapping of the spatial and temporal distribution of archaeological sites of northern China during the Neolithic and Bronze Age. Quaternary International **290,** 344-357 (2013).

51. M. Wagner et al., Radiocarbon-dated archaeological record of early first millennium BC mounted pastoralists in the Kunlun Mountains, China. Proceedings of the National Academy of Sciences **108,** 15733-15738 (2011).

52. Z. H. Tan, C. C. Huang, J. L. Pang, Q. Y. Zhou, Charcoal recorded Holocene fire history in the northern part of the Longdong Loess Plateau. Quaternary Sciences (in Chinese) **28**, 733-738 (2008).

53. J. B. Iriartea et al., Fire-free land use in pre-1492 Amazonian savannas. Proceedings of the National Academy of Sciences **109**, 6473-6478 (2012).

54. M. Moros et al., Sea surface temperatures and ice rafting in the Holocene North Atlantic: climate influences on Northern Europe and Greenland. Quaternary Science Reviews **23,** 2113-2126 (2004).

55. B. Risebrobakken, E. Jansen, C. Andersson, E. Mjelde, K. Hevroy, A high-resolution study of Holocene paleoclimatic and paleoceanographic changes in the Nordic Seas. Paleoceanography **18**, 10171 (2003).

56. G. Bond et al., A pervasive millennial-scale cycle in North Atlantic Holocene and glacial climates. Science **278,** 1257-1266 (1997).

57. H. Goosse, H. Renssen, F. M. Selten, R. J. Haarsma, J. D. Opsteegh, Potential causes of abrupt climate events: A numerical study with a three-dimensional climate model. Geophysical Research Letters **29**, 7-1-7-4 (2002).

58. M. Stuiver et al., INTCAL98 radiocarbon age calibration, 24,000-0 cal BP. Radiocarbon **40,** 1041-1083 (1998).

59. P. Zhang et al., A Test of Climate, Sun, and Culture Relationships from an 1810-Year Chinese Cave Record. Science **322,** 940-942 (2008).

60. Q. Pei, D. D. Zhang, H. F. Lee, Contextualizing human migration in different agro-ecological zones in ancient China. Quaternary International **426,** 65-74 (2016).

61. J. Ge, History of Chinese Population, Fudan University Press (in Chinese), Volumes 1-3 (2002).

62. E. Dietze et al., Holocene fire activity during low-natural flammability periods reveals scale-dependent cultural human-fire relationships in Europe. Quaternary Science Reviews **201**, 44-56 (2018).

63. O. Pechony, D. T. Shindell, Driving forces of global wildfires over the past millennium and the forthcoming century. Proceedings of the National Academy of Sciences **107**, 19167-19170 (2010).

64. V. A. Carter et al., Holocene-scale fire dynamics of central European temperate spruce-beech forests. Quaternary Science Reviews **191**, 15-30 (2018).

65. C. I. Roos, M. N. Zedeño, K. L. Hollenback, M. M. H. Erlick, Indigenous impacts on North American Great Plains fire regimes of the past millennium. Proceedings of the National Academy of Sciences **115**, 8143-8148 (2018).

66. Y. Fan, Houhanshu, Zhonghua Book Company (in Chinese), Volumes 19-23 (445).

67. China Coal Journal Editorial Committee, China Coal Journal: Comprehensive Volume. Coal Publishing House (Beijing), Volumes 1-20 (1999).

68. J. Hua, Ancient Chinese metal technology: Copper and iron civilization, Elephant Press (in Chinese), 32-318 (1999).

69. D. Zhao, General History of Chinese Economy, Hunan Press (in Chinese), Volumes 1-8 (2002).

70. X. Wu, The basic context of the history of ancient coal mines in China and the main features of coal development and utilization. Journal of China University of Mining and Technology - Social Science Edition (in Chinese) **12**, 91-98 (2010).

Figures

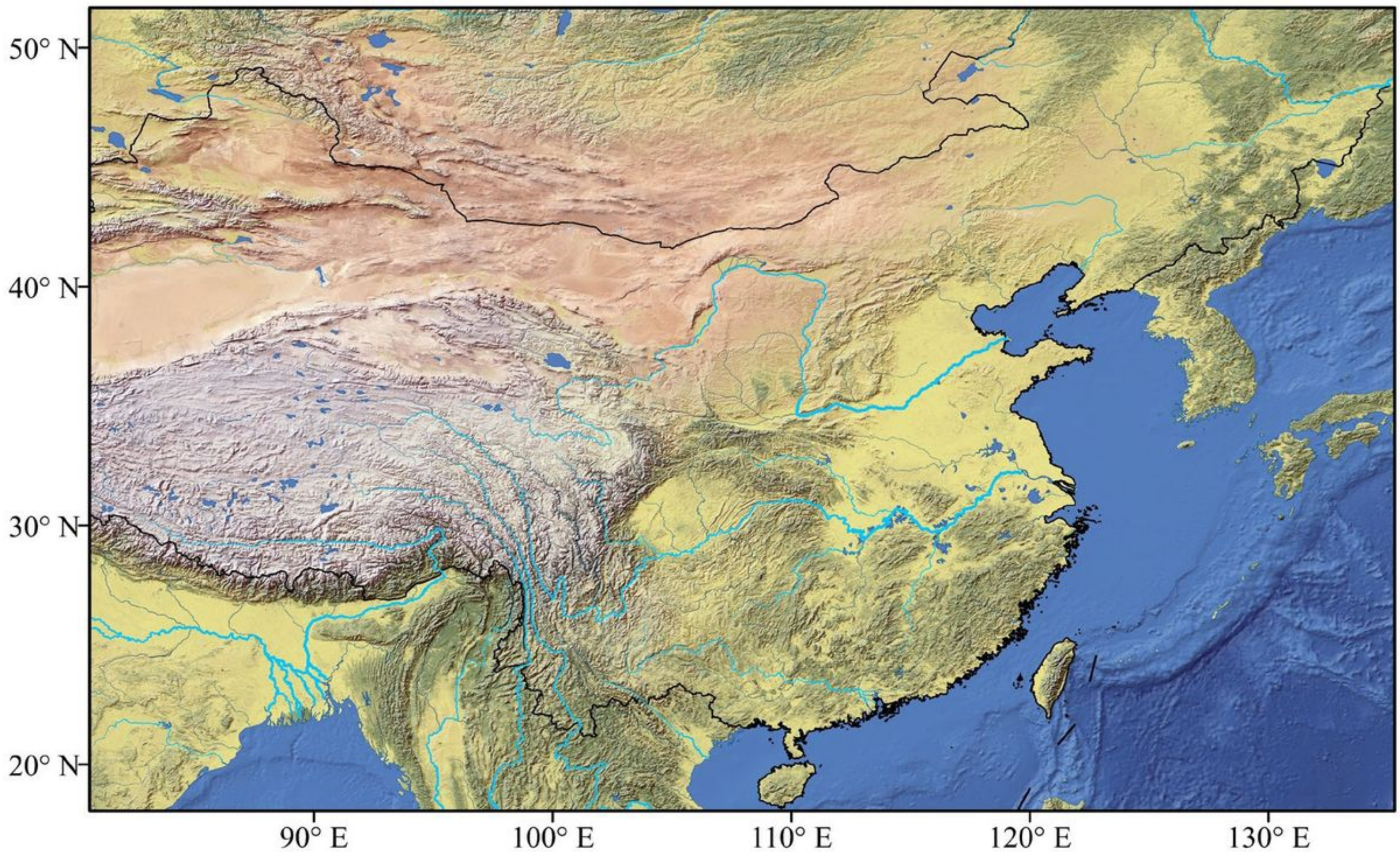

Figure 1

A map showing the winter and summer monsoons, Bohai Sea (BS), South Yellow Sea (SYS), Yellow and Yangtze Rivers, Pacific Ocean, Korean (KP) and Shandong (SP) Peninsulas, ZY2 sediment core (red circle), and locations of fire-record sediment core studied previously (yellow circles) (20, 21, 22).Note: The designations employed and the presentation of the material on this map do not imply the expression of any opinion whatsoever on the part of Research Square concerning the legal status of any country, territory, city or area or of its authorities, or concerning the delimitation of its frontiers or boundaries. This map has been provided by the authors.

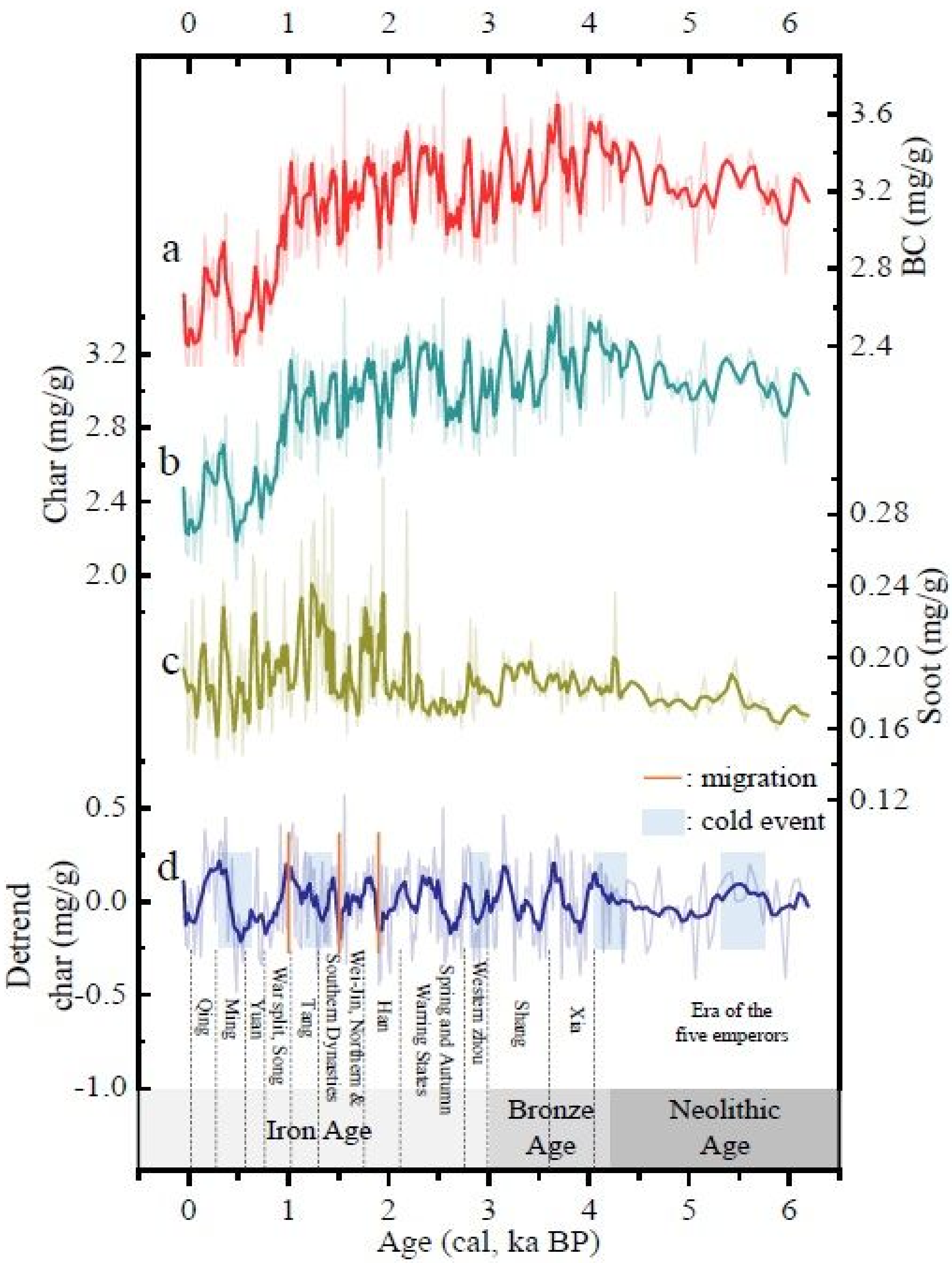

Figure 2

Sediment BC data for core ZY2 since ~6.2 ka BP: the variation in (a) BC, (b) char, and (c) soot; (d) the char detrend with 50% loess regression (Fig. S1). Signal smoothing averaging three adjacent points for (a) to (c), and seven points for (d).

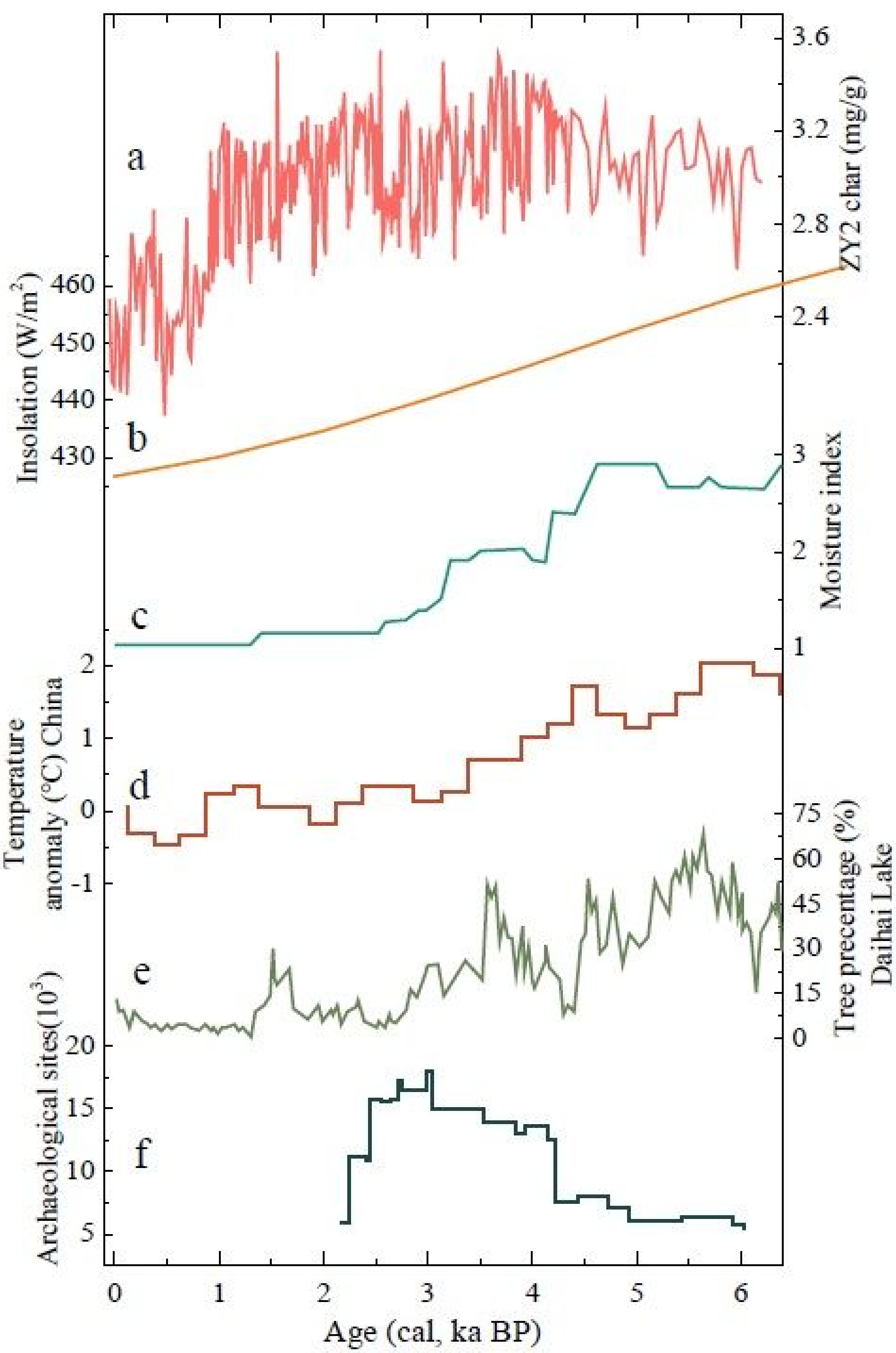

Figure 3

Comparison of the millennial-timescale variation in BC records from ZY2 with other records since 6.2 ka BP. (a) Fire activities recorded by char from core ZY2 in the SYS (this study); (b) extraterrestrial insolation of mid-month insolation 65N for July (33); (c) moisture index-based pollen in northern China (39); (d) temperature anomaly in China (38); (e) percentage of tree pollen recorded from the sediment core in Lake Daihai (40); (f) change in the total number of archaeological sites in northern China from 6 to 2 ka BP (50).

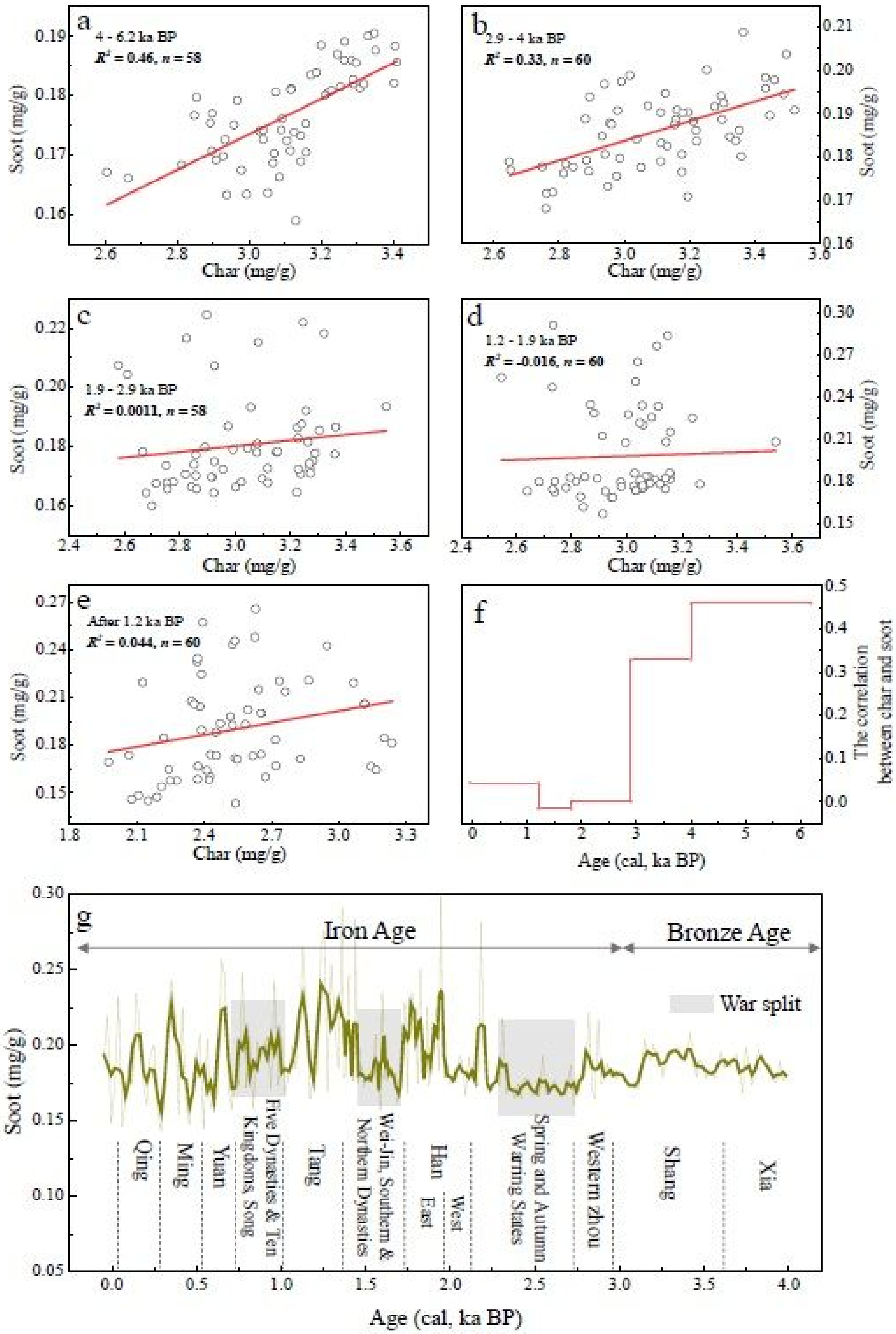

Figure 4

(a) to (e) show the correlations between char and soot at 0.05–1.2, 1.2–1.88, 1.88–2.9, 2.9–4, and, 4–6.2 ka BP, respectively. (f) Change in the correlation between char and soot since ~6.2 ka BP; (g) changes in soot from 0 to 4 ka BP and the corresponding Chinese dynasties; signal smoothing was performed by averaging three adjacent points.

Supplementary Files